PHYSICS

Superconductivity in infinite-layer nickelate $La_{1-x}Ca_xNiO_2$ thin films

Shengwei Zeng[1]*†, Changjian Li[2,3]†, Lin Er Chow[1]†, Yu Cao[4], Zhaoting Zhang[1], Chi Sin Tang[5,6], Xinmao Yin[7], Zhi Shiuh Lim[1], Junxiong Hu[1], Ping Yang[2,5], Ariando Ariando[1]*

We report the observation of superconductivity in infinite-layer Ca-doped $LaNiO_2$ ($La_{1-x}Ca_xNiO_2$) thin films and construct their phase diagram. Unlike the metal-insulator transition in Nd- and Pr-based nickelates, the undoped and underdoped $La_{1-x}Ca_xNiO_2$ thin films are entirely insulating from 300 K down to 2 K. A superconducting dome is observed at $0.15 < x < 0.3$ with weakly insulating behavior at the overdoped regime. Moreover, the sign of the Hall coefficient R_H changes at low temperature for samples with a higher doping level. However, distinct from the Nd- and Pr-based nickelates, the R_H-sign-change temperature remains at around 35 K as the doping increases, which begs further theoretical and experimental investigation to reveal the role of the 4f orbital to the (multi) band nature of the superconducting nickelates. Our results also emphasize a notable role of lattice correlation on the multiband structures of the infinite-layer nickelates.

INTRODUCTION

The resemblance of the high critical temperature (high-T_c) superconducting cuprates in the nickel-based compounds has made superconductivity in the nickelates to be one of the holy grails in superconducting research in the past three decades. The recent discovery of superconductivity in infinite-layer Sr-doped $NdNiO_2$ (*1*) has now further propelled the importance of nickelates as a route toward understanding and a material platform for searching for new high-T_c superconductors (*1*–*6*). The perovskite nickelates $RNiO_3$ (R = rare-earth element) show a structural transition and exhibit a metal-insulator transition upon cooling when R = Nd and Pr, while it remains metallic when R = La (*7*). To mimic the cuprate-like $3d^9$ electronic configuration, the infinite-layer $LaNiO_2$ is required and can be realized by oxygen deintercalation of the $LaNiO_3$ precursor (*8*). Much effort has been devoted to dope carriers in this $LaNiO_2$, but it failed to obtain superconductivity (*1*). To increase the electronic bandwidth, the La was substituted by a rare-earth element with a smaller ionic radius (e.g., Nd atom), resulting in the observation of superconductivity in $Nd_{0.8}Sr_{0.2}NiO_2$ (*1*). This route to superconductivity contrasts the heavily studied copper- and iron-based superconductors in which superconductivity was first obtained in La-based compounds (*9*, *10*), while up to now, the superconducting nickelate has only been observed in Sr-doped compounds with R = Nd or Pr (i.e., $R_{1-x}Sr_xNiO_2$) (*1*, *11*–*20*). Moreover, the trilayer nickelate $R_4Ni_3O_8$ (R = La and Pr) that has the same NiO_2 square plane as in the infinite-layer nickelates and an effective one-third hole doping showed an insulating ground state in the case of $La_4Ni_3O_8$, in contrast to the metallic state in the $Pr_4Ni_3O_8$ (*21*). Theoretical calculation attributed the absence of superconductivity to the intercalation of H atoms in energetically favorable $LaNiO_2$ to form $LaNiO_2H$ during the reduction process (*22*). It has also been shown that hybridization with Nd 4f orbitals is a non-negligible ingredient for the superconductivity in doped $NdNiO_2$, while the f orbitals are far from the Fermi level in $LaNiO_2$ (*23*–*25*). On the other hand, while earlier density functional theory (DFT) studies for $NdNiO_2$ treated the 4f orbitals as a "frozen core" under the assumption that the 4f orbitals are localized and do not show around the Fermi level (*26*, *27*), a recent DFT combined with dynamical mean-field theory calculation comparing nickelates with and without 4f orbitals also concluded that 4f orbitals are not essential to superconductivity in nickelates (*28*). This suggests the importance of elucidating the role of 4f state of the electronic structure in the occurrence of superconductivity in nickelates (*23*–*25*). Therefore, the realization of superconductivity in the La series is a key step to understanding the superconducting properties in the nickelates.

In unconventional superconductors containing the rare-earth element, the substitution of an isovalent ion with a smaller radius causes an increase in inner chemical pressure due to the shrinkage of the crystal lattice. This is considered an important method to enhance T_c, as experimentally demonstrated in cuprates and pnictides (*29*, *30*). In the Nd- and Pr-based nickelates, the Hall coefficient R_H–sign-change temperature varies with Sr doping level, indicating that the Sr doping not only introduces charges but also modulates the band structures (*4*, *11*, *12*, *15*, *31*–*33*). Moreover, the lattice constant increases with increasing Sr doping level, and the superconducting dome occurs near the R_H-sign-change boundary. It is therefore anticipated to induce superconductivity in $LaNiO_2$ through doping with a smaller ionic radius. Here, we present the observation of superconductivity in infinite-layer $La_{1-x}Ca_xNiO_2$ thin films through Ca doping.

RESULTS

Doping-dependent structural properties

The perovskite $La_{1-x}Ca_xNiO_3$ precursor thin films were synthesized by a pulsed laser deposition (PLD) technique and reduced to an

[1]Department of Physics, Faculty of Science, National University of Singapore, Singapore 117551, Singapore. [2]Department of Materials Science and Engineering, National University of Singapore, Singapore 117575, Singapore. [3]Department of Materials Science and Engineering, Southern University of Science and Technology, Shenzhen 518055, China. [4]Department of Electrical and Computer Engineering, National University of Singapore, 4 Engineering Drive 3, Singapore 117583, Singapore. [5]Singapore Synchrotron Light Source (SSLS), National University of Singapore, Singapore 117603, Singapore. [6]Institute of Materials Research and Engineering, A*STAR (Agency for Science, Technology and Research), 2 Fusionopolis Way, Singapore 138634, Singapore. [7]Shanghai Key Laboratory of High Temperature Superconductors, Physics Department, Shanghai University, Shanghai 200444, China.
*Corresponding author. Email: ariando@nus.edu.sg (A.A.); shengwei_zeng@u.nus.edu (S.W.Z.)
†These authors contributed equally to this work.

infinite-layer phase using the soft-chemistry topotactic reduction method. The x-ray diffraction (XRD) θ-2θ patterns of the as-grown $La_{1-x}Ca_xNiO_3$ thin films can be found in fig. S1. The prominent thickness oscillations in the vicinity of the (002) peak indicate the single phase and high quality of the perovskite films. After reduction, a clear transition of the diffraction peaks is seen, confirming the transformation from the perovskite to the infinite-layer structure, as shown in Fig. 1A for a representative Ca doping level of 0.23. Figure 1B shows a high-angle annular dark-field scanning transmission electron microscopy (HAADF-STEM) image of the 17-nm $La_{0.77}Ca_{0.23}NiO_2$ thin film. A clear infinite-layer structure is observed with no obvious defect throughout the layer. Note that in $Nd_{1-x}Sr_xNiO_2$, the pure perovskite and the resultant infinite-layer structure can only survive up to ~10 nm, above which the Ruddlesden-Popper–type phase emerges (*11*, *12*, *34*). For the La-nickelate thin films, the pure infinite-layer phase is still observed for a thickness of 17 nm (Fig. 1B and fig. S1). We propose two possible explanations: (i) The lattice match between the $La_{1-x}Ca_xNiO_3$ and $SrTiO_3$ substrates is much smaller than for the $Nd_{1-x}Sr_xNiO_3$, thus allowing better growth of the parent perovskite compound. (ii) A more similar ionic size between La^{3+} and the dopant ion Ca^{2+}, as compared to Nd^{3+} versus Sr^{2+}. While the observation of a stable infinite-layer phase at a larger thickness in $La_{1-x}Ca_xNiO_2$ is still preliminary, it offers an alternative route for realizing bulk-like superconducting nickelates. In addition, while the $La_{1-x}Ca_xNiO_2$ was only recently studied, we notice high reproducibility in realizing superconductivity in the system as compared to $Nd_{1-x}Sr_xNiO_2$. Figure 1C shows the XRD θ-2θ patterns of infinite-layer $La_{1-x}Ca_xNiO_2$ thin films with different Ca doping levels x from 0 to 0.35. The (00l) peak positions slightly shift toward a higher angle as Ca dopant increases, indicating a shrinking of the c-axis lattice constants d from ~3.405 Å at $x = 0$ to ~3.368 Å at $x = 0.35$ as plotted in Fig. 1D. The evolution of d is in agreement with the empirical expectation as the cation is replaced with an atom having a smaller ionic radius. The reciprocal space mappings around the (−103) diffraction peak indicate that the films are slightly relaxed, showing the larger in-plane lattice constants compared with that of the $SrTiO_3$ substrate (Fig. 1D and fig. S2). The full width at half-maximum of the rocking curves for the (002) peaks of the infinite-layer films shows a value between 0.06° and 0.12°, supporting the high-quality thin films after reduction (fig. S3).

Electronic properties

Figure 2A shows the logarithmic-scale resistivity versus temperature (ρ-T) curves of the $La_{1-x}Ca_xNiO_2$ thin films with Ca doping level x from 0 to 0.35. For $x \leq 0.15$, the samples show insulating behavior

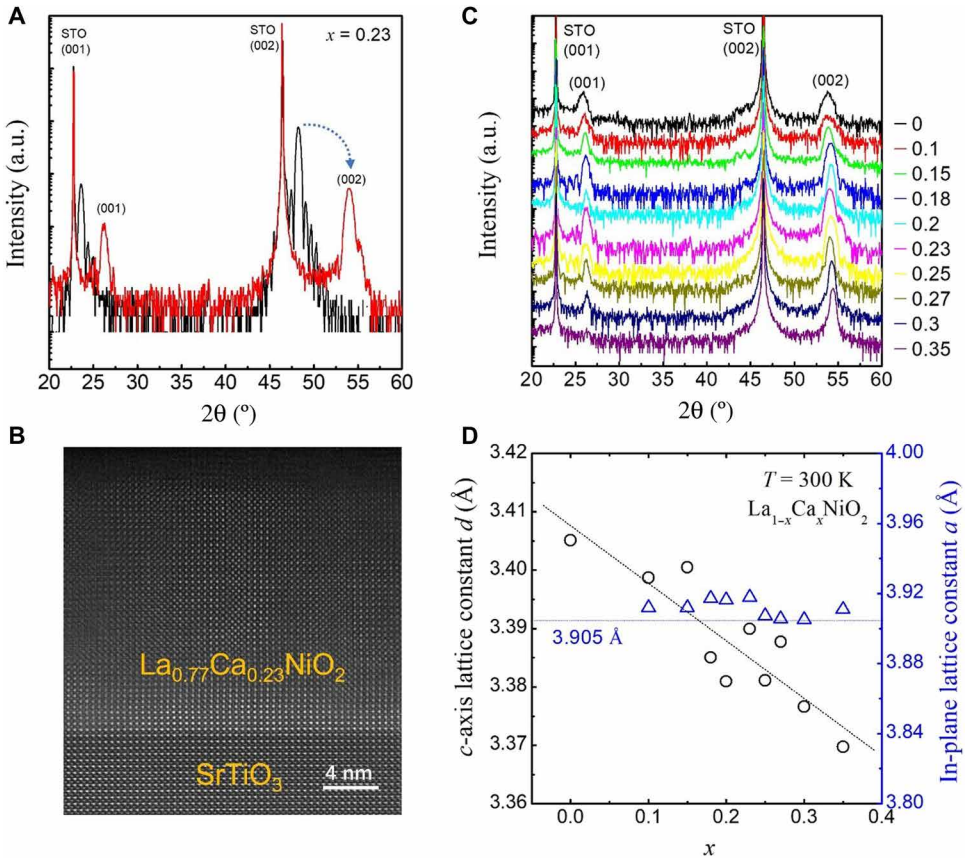

Fig. 1. Structural characterization of infinite-layer $La_{1-x}Ca_xNiO_2$ thin films. (**A**) The XRD θ-2θ intensity scan in arbitrary unit (a.u.) of the perovskite $La_{0.77}Ca_{0.23}NiO_3$ and infinite-layer $La_{0.77}Ca_{0.23}NiO_2$ thin films on a $SrTiO_3$ (STO) substrate. The arrow denotes the transition of diffraction peaks related to the transformation from a perovskite to an infinite-layer structure. (**B**) The HAADF-STEM image of the 17-nm $La_{0.77}Ca_{0.23}NiO_2$ on $SrTiO_3$ substrate. (**C**) The XRD θ-2θ scan patterns of the $La_{1-x}Ca_xNiO_2$ thin films with different Ca doping levels x. The intensity is vertically displaced for clarity. (**D**) The room-temperature c-axis lattice constants, d, and in-plane lattice constant, a, as a function of x.

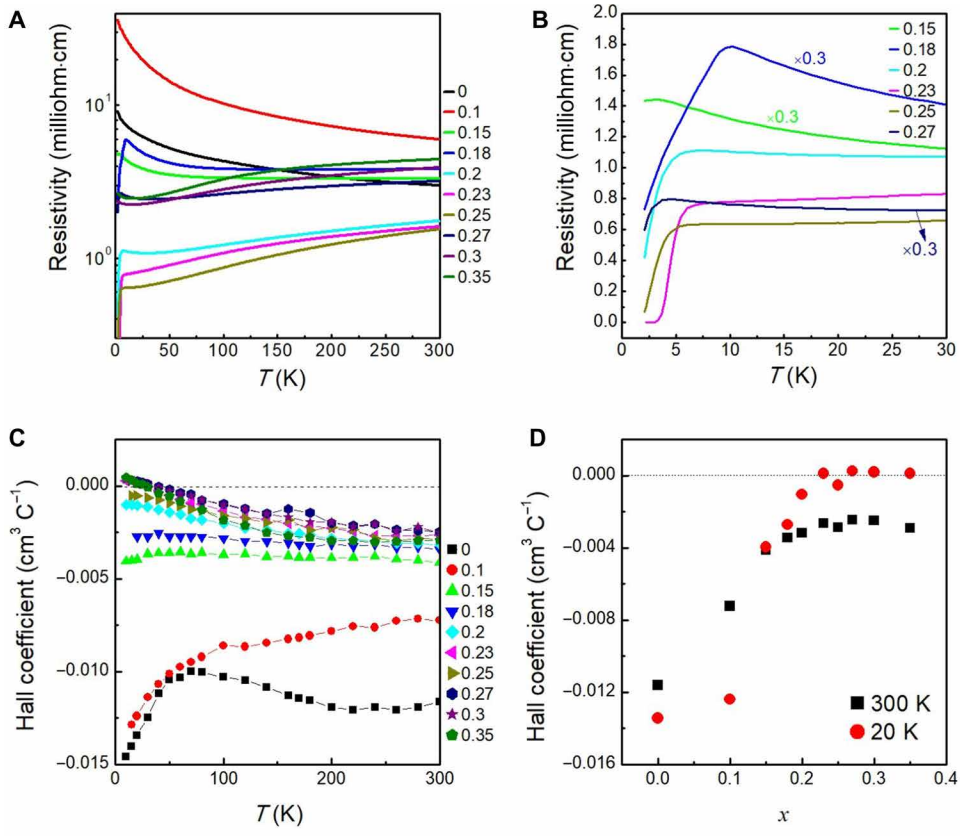

Fig. 2. Electrical transport properties of infinite-layer $La_{1-x}Ca_xNiO_2$ thin films. (**A**) The logarithmic-scale resistivity versus temperature (ρ-*T*) curves of the $La_{1-x}Ca_xNiO_2$ thin films with Ca doping level *x* from 0 to 0.35, measured from 300 to 2 K. (**B**) The zoomed-in and linear-scale ρ-*T* curves of the $La_{1-x}Ca_xNiO_2$ thin films with *x* from 0.15 to 0.27. For clarity, the resistivity of samples with $x = 0.15$, 0.18, and 0.27 is diminished to 0.3 of the initial value. (**C**) The temperature dependence of the normal-state Hall coefficients R_H. (**D**) The R_H at $T = 300$ and 20 K as a function of *x*. The dash lines are guides to the eye.

all the way below 300 K. This is different from $Nd_{1-x}Sr_xNiO_2$ and $Pr_{1-x}Sr_xNiO_2$ thin films, in which the undoped and underdoped samples show a metallic behavior at high temperatures with a resistivity minimum at the intermediate temperature below which a weakly insulating behavior appears (*1*, *11*–*13*, *15*). The high-temperature metallic behavior in undoped Nd and Pr nickelates has been thought to be due to the self-doped nature of the parent compound (*2*, *4*, *35*, *36*); however, theoretical simulations have not arrived at a dissimilar conclusion for La nickelates (*4*). The zoomed-in and linear-scale ρ-*T* curves of the superconducting $La_{1-x}Ca_xNiO_2$ thin films with *x* from 0.15 to 0.27 are shown in Fig. 2B. For $x = 0.15$ and 0.18, the samples show transitions from a slightly metallic behavior to an insulating behavior and then an onset of superconducting transition with decreasing temperature, while for $0.2 \leq x \leq 0.27$, the samples are superconducting with the ρ-*T* curves showing metallic behavior at high temperatures. The suppression of superconductivity with increasing out-of-plane magnetic field for a representative sample with $x = 0.23$ is shown in fig. S4. The fitting of the relationship between the upper critical field and midpoint critical temperature by the Ginzburg-Landau model gives the zero-temperature in-plane coherence length of 4.59 nm, comparable to that of $Nd_{0.8}Sr_{0.2}NiO_2$ film (*1*). At the overdoped regime with $x \geq 0.3$, the samples show an increase in normal state resistivity compared with that of the optimally doped sample. Moreover, similar to the Nd and Pr nickelates, the overdoped $La_{1-x}Ca_xNiO_2$ thin films exhibit weakly insulating behavior at low temperature, suggesting a universal transport property in overdoped infinite-layer nickelates (*11*, *12*, *15*).

Similar to Nd and Pr nickelates, the room temperature R_H is negative, and its magnitude decreases with increasing *x* and then saturates at $x = 0.2$ (Fig. 2, C and D), suggesting the multiband structure nature for $La_{1-x}Ca_xNiO_2$ films (*2*, *4*, *23*, *24*, *31*, *35*–*37*). The R_H remains negative below 300 K for samples with $x \leq 0.2$. For samples with $x \geq 0.23$ (except for $x = 0.25$), the R_H undergoes a smooth transition from negative to positive sign as the temperature decreases. Figure 2D presents the R_H at 20 K, clearly showing a sign change at $x = 0.2$ to 0.23 from negative to positive with increasing *x*. The doping level of the R_H sign change is higher than that ($x = 0.18$ to 0.2) of Nd and Pr nickelates (*11*, *12*, *15*). While we notice that the R_H-sign-change doping level for both La nickelates and Nd/Pr nickelates are at around the optimally doped regime, in $Nd_{1-x}Sr_xNiO_2$ and $Pr_{1-x}Sr_xNiO_2$, the R_H-sign-change temperature increases with increasing doping level (*11*, *12*, *15*). However, for $La_{1-x}Ca_xNiO_2$ films, the R_H-sign-change temperature does not change with Ca doping level, and it is at around 35 K for $x \geq 0.23$. Such distinct saturation may suggest that hole doping in the superconducting lanthanide nickelates plays a more hidden role than merely charge carrier modulation.

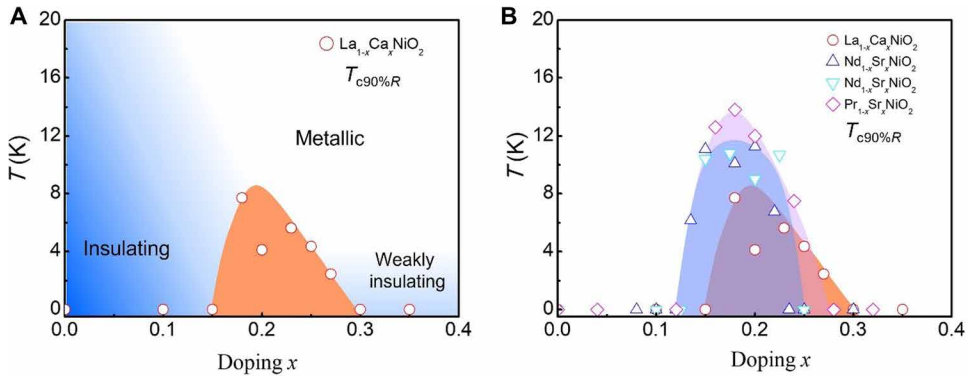

Fig. 3. Phase diagram of infinite-layer $La_{1-x}Ca_xNiO_2$ thin films and the comparison to $Nd_{1-x}Sr_xNiO_2$ and $Pr_{1-x}Sr_xNiO_2$ thin films. (**A**) The critical temperature as a function of doping level *x* for $La_{1-x}Ca_xNiO_2$ in the present results. The $T_{c,90\,\%\,R}$ is defined as the temperature at which the resistivity drops to 90% of the value at 10 K (the onset of the superconductivity). (**B**) The combined phase diagram of $La_{1-x}Ca_xNiO_2$, $Nd_{1-x}Sr_xNiO_2$, and $Pr_{1-x}Sr_xNiO_2$. The data of $Nd_{1-x}Sr_xNiO_2$ are adapted from (*11*, *12*), and the data of $Pr_{1-x}Sr_xNiO_2$ are adapted from (*15*).

Phase diagram and superconducting dome

Figure 3 depicts the phase diagrams of $La_{1-x}Ca_xNiO_2$ integrated with those of $Nd_{1-x}Sr_xNiO_2$ and $Pr_{1-x}Sr_xNiO_2$ (*11*, *12*, *15*). The onset of the critical temperature, $T_{c,90\,\%\,R}$, is defined as the temperature at which the resistivity drops to 90% of the normal-state value at the onset of the superconductivity. A superconducting dome between $0.15 < x < 0.3$ is seen for $La_{1-x}Ca_xNiO_2$. The doping range of the $La_{1-x}Ca_xNiO_2$ superconducting dome is comparable to that of $Pr_{1-x}Sr_xNiO_2$ and slightly wider than that of $Nd_{1-x}Sr_xNiO_2$ but is generally extended toward a higher doping level (Fig. 3B). At the two ends of the dome, the underdoped regime shows insulating behavior upon cooling, and the overdoped regime is weakly insulating at low temperature, different from the Nd and Pr nickelates in which both regimes show weakly insulating behavior (*11*, *12*, *15*). In general, the T_c of $La_{1-x}Ca_xNiO_2$ is lower than those of Nd and Pr series, possibly because of the large ionic radius of La, consistent with the experimental observation in Cu- and Fe-based superconductors that the T_c is enhanced as the ionic radius of the rare-earth element decreases (*29*, *30*). This observation implies that the appearance of superconductivity in infinite-layer nickelates is not reliant on the 4f electrons of the rare-earth element and suggests that higher T_c in infinite-layer nickelates can be stabilized using smaller rare-earth ions.

DISCUSSION

In addition to introducing charge carriers, the chemical doping in infinite-layer nickelates can cause the change of the multiband structures because of the modification of the lattice environment (*4*, *31*–*33*). Therefore, the normal-state properties and the superconducting range will depend on the lattice constant upon doping, which can be seen from the doping-dependent R_H and superconducting dome (*11*, *12*, *15*). Depending on the difference of cation and dopant radii, the extent of the lattice-constant change upon doping is different. In $Nd_{1-x}Sr_xNiO_2$ (*11*, *12*), the extent of the lattice-constant change with Sr doping is ~0.53 Å per one Sr atom, larger than that (~0.42 Å per one Sr atom) for $Pr_{1-x}Sr_xNiO_2$ (*15*) and that (~0.11 Å per one Ca atom) for $La_{1-x}Ca_xNiO_2$ that is observed in the current result. It is found that the superconducting dome of the $Nd_{1-x}Sr_xNiO_2$ is narrower than that of the $Pr_{1-x}Sr_xNiO_2$ and $La_{1-x}Ca_xNiO_2$, suggesting the intrinsic link between the superconducting range and the modulation of the lattice constant. Moreover, theoretical calculations suggested that Sr doping in $Nd_{1-x}Sr_xNiO_2$ reduces the self-doping effect, and the nickelate behaves more like a system with a pure single-band picture (*4*, *33*). This is consistent with the R_H sign change upon doping, and the sign-change temperature monotonically increases with increasing Sr doping level in Nd and Pr nickelates (*11*, *12*, *15*). However, for $La_{1-x}Ca_xNiO_2$ films, the doping-dependent R_H-sign-change temperature is negligible for $x \geq 0.23$. Coupled with the small change in the lattice constant, this suggests the critical role of the dopant ionic nature on the electronic modulation in infinite-layer nickelates. For the infinite-layer bulk nickelates $Nd_{1-x}Sr_xNiO_2$ and $Sm_{1-x}Sr_xNiO_2$ in which superconductivity is absent, the *c*-lattice constant is smaller than those of superconducting thin films (*38*–*40*). Moreover, we also found that the strain effect induced electronic bandstructure modulation and the resultant change of R_H in $Nd_{0.8}Sr_{0.2}NiO_2$ (*41*). At the same time as our report, superconductivity was also independently realized in (La, Sr)NiO_2 (*42*). These suggest the importance of the lattice environment on the superconductivity and normal-state properties in infinite-layer nickelates. The present result also suggests a new route for new superconductors and a unique way for tailoring normal-state properties through dopants in nickelate superconductors.

MATERIALS AND METHODS

We prepared and characterized our Ca-doped $LaNiO_2$ samples following procedures previously described in (*12*).

Sample preparation

The ceramic targets with nominal composition $La_{1-x}Ca_xNiO_3$ were prepared by the conventional solid-state reaction using high-purity La_2O_3 (99.999%; Sigma-Aldrich), NiO_2 (99.99%; Sigma-Aldrich), and $CaCO_3$ (99.995%; Sigma-Aldrich) powders as the starting materials. The mixed powders were sintered in air for 15 hours at 1150°, 1200°, and 1250°C, respectively, with thorough regrinding before each sintering. On the final sintering, the powder was pressed into a disk-shaped pellet. The perovskite thin films were grown on TiO_2-terminated (001) $SrTiO_3$ substrates using a PLD technique

with a 248-nm KrF excimer laser. The deposition temperature and oxygen partial pressure PO_2 for all samples were 600°C and 150 mtorr, respectively. The laser energy density on the target surface was set to be 1.8 J cm^{-2}. After deposition, the samples were annealed for 10 min at 600°C and 150 mtorr and then cooled down to room temperature at a rate of 8°C/min. To obtain the infinite-layer structures, the as-grown films were then embedded with about 0.15 g of CaH_2 powder and wrapped in aluminum foil and then placed into the PLD chamber for the reduction process. The wrapped sample was heated to 340 ° to 360°C at a rate of 25°C/min and kept for 80 min and then cooled down to room temperature at a rate of 25°C/min.

Electronic transport and structural characterization

The transport measurements were performed using a Quantum Design Physical Property Measurement System. The wire connection for the electrical transport measurement was made by Al ultrasonic wire bonding. The XRD measurement was done in the X-ray Diffraction and Development beamline at Singapore Synchrotron Light Source (SSLS) with an x-ray wavelength of λ = 1.5404 Å. The HAADF-STEM imaging was carried out at 200 kV with a JEOL ARM200F microscope, and the cross-sectional TEM specimens were prepared by a focused ion beam machine (FEI Versa 3D).

SUPPLEMENTARY MATERIALS

Supplementary material for this article is available at https://science.org/doi/10.1126/sciadv.abl9927

REFERENCES AND NOTES

1. D. Li, K. Lee, B. Y. Wang, M. Osada, S. Crossley, H. R. Lee, Y. Cui, Y. Hikita, H. Y. Hwang, Superconductivity in an infinite-layer nickelate. *Nature* **572**, 624–627 (2019).
2. A. S. Botana, F. Bernardini, A. Cano, Nickelate superconductors: An ongoing dialog between theory and experiments. *J. Exp. Theoretical Phys.* **132**, 618–627 (2021).
3. B. H. Goodge, D. Li, K. Lee, M. Osada, B. Y. Wang, G. A. Sawatzky, H. Y. Hwang, L. F. Kourkoutis, Doping evolution of the Mott–Hubbard landscape in infinite-layer nickelates. *Proc. Natl. Acad. Sci.* **118**, e2007683118 (2021).
4. A. S. Botana, M. R. Norman, Similarities and differences between $LaNiO_2$ and $CaCuO_2$ and implications for superconductivity. *Phys. Rev. X* **10**, 011024 (2020).
5. G. A. Sawatzky, Superconductivity seen in a non-magnetic nickel oxide. *Nature* **572**, 592–593 (2019).
6. M. Jiang, M. Berciu, G. A. Sawatzky, Critical nature of the Ni Spin state in doped $NdNiO_2$. *Phys. Rev. Lett.* **124**, 207004 (2020).
7. S. Catalano, M. Gibert, J. Fowlie, J. Íñiguez, J. M. Triscone, J. Kreisel, Rare-earth nickelates $RNiO_3$: Thin films and heterostructures. *Rep. Prog. Phys.* **81**, 046501 (2018).
8. M. A. G. M. A. Hayward, M. J. Rosseinsky, J. Sloan, Sodium hydride as a powerful reducing agent for topotactic oxide deintercalation-synthesis and characterization of the Nickel(I) Oxide $LaNiO_2$. *J. Am. Chem. Soc.* **121**, 8843–8854 (1999).
9. J. G. Bednorz, K. A. Müller, Possible highT c superconductivity in the Ba–La–Cu–O system. *Z. Phys. B. Condens. Matter* **64**, 189–193 (1986).
10. Y. Kamihara, T. Watanabe, M. Hirano, H. Hosono, Iron-based layered superconductor $La[O_{1-x}F_x]FeAs$ (x = 0.05− 0.12) with T_c= 26 K. *J. Am. Chem. Soc.* **130**, 3296–3297 (2008).
11. D. Li, B. Y. Wang, K. Lee, S. P. Harvey, M. Osada, B. H. Goodge, L. F. Kourkoutis, H. Y. Hwang, Superconducting dome in $Nd_{1-x}Sr_xNiO_2$ infinite layer films. *Phys. Rev. Lett.* **125**, 027001 (2020).
12. S. Zeng, C. S. Tang, X. Yin, C. Li, M. Li, Z. Huang, J. Hu, W. Liu, G. J. Omar, H. Jani, Z. S. Lim, K. Han, D. Wan, P. Yang, S. J. Pennycook, A. T. S. Wee, A. Ariando, Phase diagram and superconducting dome of infinite-layer $Nd_{1-x}Sr_xNiO_2$ thin films. *Phys. Rev. Lett.* **125**, 147003 (2020).
13. M. Osada, B. Y. Wang, B. H. Goodge, K. Lee, H. Yoon, K. Sakuma, D. Li, M. Miura, L. F. Kourkoutis, H. Y. Hwang, A superconducting praseodymium nickelate with infinite layer structure. *Nano Lett.* **20**, 5735–5740 (2020).
14. Q. Gu, Y. Li, S. Wan, H. Li, W. Guo, H. Yang, Q. Li, X. Zhu, X. Pan, Y. Nie, H. H. Wen, Single particle tunneling spectrum of superconducting $Nd_{1-x}Sr_xNiO_2$ thin films. *Nat. Commun.* **11**, 6027 (2020).
15. M. Osada, B. Y. Wang, K. Lee, D. Li, H. Y. Hwang, Phase diagram of infinite layer praseodymium nickelate $Pr_{1-x}Sr_xNiO_2$ thin films. *Phys. Rev. Mater.* **4**, 121801 (2020).
16. Q. Gao, Y. Zhao, X. Zhou, Z. Zhu, Preparation of superconducting thin film of infinite-layer nickelate $Nd_{0.8}Sr_{0.2}NiO_2$. arXiv:2102.10292 [cond-mat.supr-con] (20 February 2021).
17. X.-R. Zhou, Z.-X. Feng, P.-X. Qin, H. Yan, X.-N. Wang, P. Nie, H.-J. Wu, X. Zhang, H.-Y. Chen, Z.-A. Meng, Z.-W. Zhu, Z.-Q. Liu, Negligible oxygen vacancies, low critical current density, electric-field modulation, in-plane anisotropic and high-field transport of a superconducting $Nd_{0.8}Sr_{0.2}NiO_2/SrTiO_3$ heterostructure. *Rare Metals* **40**, 2847–2854 (2021).
18. B. Y. Wang, D. Li, B. H. Goodge, K. Lee, M. Osada, S. P. Harvey, L. F. Kourkoutis, M. R. Beasley, H. Y. Hwang, Isotropic Pauli-limited superconductivity in the infinite-layer nickelate $Nd_{0.775}Sr_{0.225}NiO_2$. *Nat. Phys.* **17**, 473–477 (2021).
19. H. Lu, M. Rossi, A. Nag, M. Osada, D. F. Li, K. Lee, B. Y. Wang, M. Garcia-Fernandez, S. Agrestini, Z. X. Shen, E. M. Been, B. Mortiz, T. P. Devereaux, J. Zaaneh, H. Y. Hwang, K.-J. Zhou, W. S. Lee, Magnetic excitations in infinite-layer nickelates. *Science* **373**, 213–216 (2021).
20. P. Puphal, Y.-M. Wu, K. Fürsich, H. Lee, M. Pakdaman, Jan AN Bruin, J. Nuss, Y Eren Suyolcu, Peter A van Aken, B. Keimer, M. Isobe, M. Hepting, Topotactic transformation of single-crystals: From perovskite to infinite-layer nickelates. arXiv:2106.13171 [cond-mat.supr-con] (24 June 2021).
21. J. Zhang, A. S. Botana, J. W. Freeland, D. Phelan, H. Zheng, V. Pardo, M. R. Norman, J. F. Mitchell, Large orbital polarization in a metallic square-planar nickelate. *Nat. Phys.* **13**, 864–869 (2017).
22. L. Si, W. Xiao, J. Kaufmann, J. M. Tomczak, Y. Lu, Z. Zhong, K. Held, Topotactic hydrogen in nickelate superconductors and akin infinite-layer oxides ABO_2. *Phys. Rev. Lett.* **124**, 166402 (2020).
23. P. Jiang, L. Si, Z. Liao, Z. Zhong, Electronic structure of rare-earth infinite-layer $RNiO_2$ (R= La, Nd). *Phys. Rev. B* **100**, 201106(R) (2019).
24. M.-Y. Choi, K.-W. Lee, W. E. Pickett, Role of 4f states in infinite-layer $NdNiO_2$. *Phys. Rev. B* **101**, 020503(R) (2020).
25. S. Bandyopadhyay, P. Adhikary, T. Das, I. Dasgupta, T. Saha-Dasgupta, Superconductivity in infinite-layer nickelates: Role of f orbitals. *Phys. Rev. B* **102**, 220502 (2020).
26. Y. Nomura, M. Hirayama, T. Tadano, Y. Yoshimoto, K. Nakamura, R. Arita, Formation of a two-dimensional single-component correlated electron system and band engineering in the nickelate superconductor $NdNiO_2$. *Phys. Rev. B* **100**, 205138 (2019).
27. X. Wu, D. Di Sante, T. Schwemmer, W. Hanke, H. Y. Hwang, S. Raghu, R. Thomale, Robust $d_{x^2-y^2}$-wave superconductivity of infinite-layer nickelates. *Phys. Rev. B* **101**, 060504(R) (2020).
28. Z. Liu, C. Xu, C. Cao, W. Zhu, Z. F. Wang, J. Yang, Doping dependence of electronic structure of infinite-layer $NdNiO_2$. *Phys. Rev. B* **103**, 045103 (2021).
29. H. Hosono, K. Kuroki, Iron-based superconductors: Current status of materials and pairing mechanism. *Physica C* **514**, 399–422 (2015).
30. N. P. Armitage, P. Fournier, R. L. Greene, Progress and perspectives on electron-doped cuprates. *Rev. Mod. Phys.* **82**, 2421–2487 (2010).
31. J. Gao, Z. Wang, C. Fang, H. Weng, Electronic structures and topological properties in nickelates $Ln_{n+1}Ni_nO_{2n+2}$. *Natl. Sci. Rev.* **8**, nwaa218 (2021).
32. F. Lechermann, Doping-dependent character and possible magnetic ordering of $NdNiO_2$. *Phys. Rev. Mater.* **5**, 044803 (2021).
33. M. Kitatani, L. Si, O. Janson, R. Arita, Z. Zhong, K. Held, Nickelate superconductors—A renaissance of the one-band Hubbard model. *npj Quant. Mater.* **5**, 59 (2020).
34. K. Lee, B. H. Goodge, D. Li, M. Osada, B. Y. Wang, Y. Cui, L. F. Kourkoutis, H. Y. Hwang, Aspects of the synthesis of thin film superconducting infinite-layer nickelates. *APL Mater.* **8**, 041107 (2020).
35. G.-M. Zhang, Y.-f. Yang, F.-C. Zhang, Self-doped Mott insulator for parent compounds of nickelate superconductors. *Phys. Rev. B* **101**, 020501(R) (2020).
36. M. Hepting, D. Li, C. J. Jia, H. Lu, E. Paris, Y. Tseng, X. Feng, M. Osada, E. Been, Y. Hikita, Y. D. Chuang, Z. Hussain, K. J. Zhou, A. Nag, M. Garcia-Fernandez, M. Rossi, H. Y. Huang, D. J. Huang, Z. X. Shen, T. Schmitt, H. Y. Hwang, B. Moritz, J. Zaanen, T. P. Devereaux, W. S. Lee, Electronic structure of the parent compound of superconducting infinite-layer nickelates. *Nat. Mater.* **19**, 381–385 (2020).
37. K.-W. Lee, W. Pickett, Infinite-layer $LaNiO_2$: Ni^{1+} is not Cu^{2+}. *Phys. Rev. B* **70**, 165109 (2004).
38. Q. Li, C. He, J. Si, X. Zhu, Y. Zhang, H. H. Wen, Absence of superconductivity in bulk $Nd_{1-x}Sr_xNiO_2$. *Commun. Mater.* **1**, 16 (2020).
39. B.-X. Wang, H. Zheng, E. Krivyakina, O. Chmaissem, P. P. Lopes, J. W. Lynn, L. C. Gallington, Y. Ren, S. Rosenkranz, J. F. Mitchell, D. Phelan, Synthesis and characterization of bulk $Nd_{1-x}Sr_xNiO_2$ and $Nd_{1-x}Sr_xNiO_3$. *Phys. Rev. Mater.* **4**, 084409 (2020).
40. C. He, X. Ming, Q. Li, X. Zhu, J. Si, H.-H. Wen, Synthesis and physical properties of perovskite $Sm_{1-x}Sr_xNiO_3$ (x = 0, 0.2) and infinite-layer $Sm_{1-x}Sr_xNiO_2$ nickelates. *J. Phys. Condens. Matter* **33**, 265701 (2021).
41. S. Zeng, X. M. Yin, C. J. Li, C. S. Tang, K. Han, Z. Huang, Y. Cao, L. E. Chow, D. Y. Wan, Z. T. Zhang, Z. S. Lim, C. Z. Diao, P. Yang, A. T. S. Wee, S. J. Pennycook, A. Ariando, Observation of perfect diamagnetism and interfacial effect on the electronic structures in infinite-layer superconducting $Nd_{0.8}Sr_{0.2}NiO_2$ superconducting infinite layers. arXiv:2104.14195 [cond-mat.supr-con] (29 April 2021).

42. M. Osada, B. Y. Wang, B. H. Goodge, S. P. Harvey, K. Lee, D. Li, L. F. Kourkoutis, H. Y. Hwang, Nickelate superconductivity without rare-earth magnetism:(La, Sr)NiO_2. *Adv. Mater.* **33**, 2104083 (2021).

Acknowledgments

Funding: This research is supported by the Agency for Science, Technology, and Research (A*STAR) under its Advanced Manufacturing and Engineering (AME) Individual Research Grant (IRG) (A1983c0034). S.W.Z., C.J.L., Y.C., and A.A. also acknowledge the partial support from the Ministry of Education (MOE) of Singapore under the Tier 2 Grant (Project no. T2EP50121-0039) and the Singapore National Research Foundation (NRF) under the Competitive Research Programs (CRP grant no. NRF-CRP15-2015-01). P.Y. is supported by the SSLS via NUS Core Support C-380-003-003-001. The authors would also like to acknowledge the SSLS for providing the facility necessary for conducting the research. The Laboratory is a National Research Infrastructure under the National Research Foundation (NRF) Singapore. **Author contributions:** S.W.Z. and A.A. conceived the project. S.W.Z., L.E.C., Y.C., Z.T.Z., Z.S.L., and J.X.H. prepared the thin films and conducted the electrical measurements. S.W.Z., P.Y., C.S.T., and X.M.Y. conducted the XRD measurements. C.J.L. conducted the STEM measurements. S.W.Z. and A.A. wrote the manuscript with contributions from all authors. All authors have discussed the results and the interpretations. **Competing interests:** The authors declare that they have no competing interests. **Data and materials availability:** All data needed to evaluate the conclusions in the paper are present in the paper and/or the Supplementary Materials.

Submitted 18 August 2021
Accepted 23 December 2021
Published 18 February 2022
10.1126/sciadv.abl9927